Crop and Environment 1 (2022) 119–132

Contents lists available at ScienceDirect

Crop and Environment

journal homepage: www.journals.elsevier.com/crop-and-environment

Original Article

Estimating photosynthetic parameter values of rice, wheat, maize and sorghum to enable smart crop cultivation

Dong Wang [a,b], Winda Rianti [a,c], Fabián Gálvez [a,d], Peter E.L. van der Putten [a], Paul C. Struik [a], Xinyou Yin [a,*]

[a] Centre for Crop Systems Analysis, Department of Plant Sciences, Wageningen University & Research, P.O. Box 430, 6700 AK Wageningen, the Netherlands
[b] Shanghai Lankuaikei Technology Development Co. Ltd., No. 888 Huanhu West 2nd Road, Pudong New District, Shanghai, China
[c] Faculty of Agriculture, Universitas Singaperbangsa, Karawang, 41361, Indonesia
[d] Faculty of Life Sciences, Polytechnic Superior School of Litoral (ESPOL), Campus Gustavo Galindo Velasco, Km 30.5 Perimetral Road, P.O. Box 09-01-5863, Guayaquil, Ecuador

ARTICLE INFO

Keywords:
C_3
C_4
Leaf nitrogen content
Photosynthesis model
Photosynthesis parameters

ABSTRACT

Crop models can support the design of smart crop management practices. The Farquhar-von Caemmerer-Berry (FvCB) model is increasingly being used in these models for quantifying leaf photosynthesis. Nitrogen (N) is required for many functional machineries of photosynthesis, thus relationships between FvCB-model parameters and leaf N content (LNC) should be established. We conducted combined gas exchange and chlorophyll fluorescence measurements on fully expanded leaves of two C_3 crops, rice (*Oryza sativa*) and wheat (*Triticum aestivum*), and two C_4 crops, maize (*Zea mays*) and sorghum (*Sorghum bicolor*), grown under three N levels. Photosynthetic parameters were estimated and linear relationships between these parameters and LNC were quantified in both C_3 and C_4 crop types. The efficiency of converting incident light into linear electron transport for C_3 crops or into ATP production for C_4 crops showed a weak increase with LNC. The maximum electron transport rate (J_{max}) for C_3 crops or the maximum ATP production rate ($J_{max,atp}$) for C_4 crops significantly increased with LNC. The increase in Rubisco carboxylation capacity (V_{cmax}) with LNC was significantly higher in C_3 than in C_4 crops. Triose phosphate utilization for C_3 crops and PEP carboxylation capacity (V_{pmax}) for C_4 crops increased significantly with LNC as well. Except for J_{max} at 21% O_2 and V_{cmax} of C_3 crops, there was no significant difference among crops in the relationship between estimated photosynthetic parameters and LNC. The tight associations of photosynthesis parameters with LNC were discussed in view of decision making on N management in the context of smart farming.

1. Introduction

Breeding semi-dwarf crop cultivars in the 1960s that could benefit from an increase in inputs of fertilizer, irrigation water and pesticides has resulted in the first Green Revolution (Bailey-Serres et al., 2019; Pingali, 2012). Achieving further food security to meet demands for ever growing populations in a sustainable way requires high yields and efficient resource use, a great challenge for modern agriculture. Smart farming is key to fulfilling this challenge in sustainable agriculture (Walter et al., 2017). Smart farming entails smart crop cultivation tailored to specific crops grown under specific conditions.

Smart crop cultivation requires in-season adaptive management, based on crop yield forecasting that is conditional on the status of crop, water, and nutrients in the cropping systems. Together with the development of unmanned aerial vehicles, the exploitation of remote and proximal sensing apparatus has become a key to sophisticated *in situ* smart crop cultivation in open fields (Walter et al., 2017). For instance, site-specific crop growth and nitrogen (N) status have been retrieved from multi- or hyper-spectral images recently (Hank et al., 2019). However, there is a huge phenotypic gap between retrieved-N and crop yield. Crop models have long been developed based on crop physiological principles and used to predict crop growth and yield in response to various environmental variables (including N supply), and thus may serve as a tool to bridge the gap. As photosynthesis is the primary physiological process in crop production (Lawlor, 1995) and is very sensitive to environmental conditions and crop management, an accurate

* Corresponding author.
E-mail address: xinyou.yin@wur.nl (X. Yin).

https://doi.org/10.1016/j.crope.2022.05.004
Received 19 December 2021; Received in revised form 3 May 2022; Accepted 6 May 2022

and robust modelling of photosynthesis or related parameters is a prerequisite for crop models in predicting crop growth and yield. Ambient weather conditions, including solar radiation, air temperature, humidity and CO_2 concentration, have a direct impact on crop photosynthesis. Agronomic management practices, such as fertilization can also affect the crop's photosynthetic performance, because they affect canopy development and the photosynthetic proteins' contents, and thus light capture and gas exchange (McDowell, 2011). Similarly, rainfall and irrigation determine the soil water balance, thereby indirectly affecting crop photosynthesis. Crop protection also plays a significant role in maintaining crop photosynthesis and growth.

Based on their approach of simulating the process of photosynthesis, crop models can be classified into three categories (Li et al., 2015): models based on the canopy radiation use efficiency (RUE) (Monteith, 1977), models utilizing the light-response curve of single-leaf photosynthesis and integrating it to the canopy level (de Wit, 1978), and models describing the photosynthetic process *via* the biochemical model of Farquhar et al. (1980) ("the FvCB model", hereafter) and upscaling it from leaf to canopy. The RUE concept is used in many crop models (Boote et al., 1996) and works fairly well under many conditions (Sinclair and Rawlins, 1993). However, RUE is a composite parameter that depends not only on species-related biosynthesis products and photosynthesis type (Kiniry et al., 1989), but also on leaf physiological status (e.g. N content) and environmental factors (e.g. temperature, radiation, and water stress intensity) affecting leaf photosynthetic rate (Sinclair and Horie, 1989; Sinclair and Muchow, 1999). Without the specific prediction of photosynthetic processes describing an effective RUE, models based on RUE are hardly convincing under nonoptimal conditions (Boote et al., 1996), because these crop models lack appropriate algorithms to describe the effects of complex interactions between multiple environmental and physiological factors on RUE (Yin et al., 2021b). As for the simple light response models, although the photosynthesis can be upscaled from leaf to canopy, the interaction effects of multiple factors on leaf-photosynthesis parameters have not been modelled adequately (Yin et al., 2021b). The FvCB model is based on the understanding of the major biochemical component processes of photosynthesis. Its further developments and extensions have been reviewed recently by Yin et al. (2021a). Because of its mechanistic level and simplicity, the FvCB model has been widely used not only for analyzing leaf biochemistry and quantifying leaf photosynthesis responses under different environmental conditions (Bernacchi et al., 2001, 2003), but also for upscaling to project productivities of canopies and ecosystems and to model global carbon fluxes responding to environmental changes (Rogers, 2014).

The FvCB model predicts the net leaf photosynthetic rate (A) of C_3 species as the minimum of the Rubisco-limited (A_c) and electron (e^-) transport-limited (A_j) rate of photosynthesis (Farquhar et al., 1980). The model for both A_c and A_j accounts for the CO_2 released through photorespiration, in which oxygenation of ribulose bisphosphate is innately linked to its carboxylation by Rubisco and potentially reduces the rate of photosynthesis by over 20% (Ehleringer et al., 1991). Later, it was modified by adding a third limitation set by triose phosphate utilization (TPU), in which A may be ceiled by the rate as determined by the export of triose phosphate (A_p) (Herold, 1980). Maximum rates of these three limited processes are determined by Rubisco carboxylation capacity (V_{cmax}), e^- transport capacity (J_{max}), and rate of TPU (T_p), respectively.

Compared with C_3 photosynthesis, C_4 photosynthesis is more complicated because of its operation of the additional CO_2 concentrating mechanism (CCM) cycle, also called C_4 cycle, prior to the C_3 cycle as occurring in C_3 photosynthesis. In C_4 photosynthesis, CO_2 is firstly converted into bicarbonate which is fixed by phosphoenolpyruvate (PEP) carboxylase (PEPc) into C_4-acids in thin-walled mesophyll cells. Then these C_4-acids are transported to thick-walled bundle sheath cells, in which C_4-acids are decarboxylated. The released CO_2 is re-fixed via Rubisco in the C_3 cycle. As PEPc has a high affinity to bicarbonate and a likely higher maximal velocity than Rubisco, the C_4 cycle runs faster than the C_3 cycle. This results in CO_2 concentrations in bundle sheath cells that are 10- to 20-fold higher than in the mesophyll cells. Therefore, photorespiration is suppressed in C_4 photosynthesis and this improves the carboxylation efficiency of Rubisco (Osmond et al., 1982). An FvCB-type C_4 photosynthesis model was developed (von Caemmerer and Furbank, 1999), assuming that reactions of both C_4 and C_3 cycles are limited by either enzyme activity or e^- transport. Yin et al. (2011b) revised this C_4 model, considering that either cycle can be limited by enzyme activity or by e^- transport, and thus there are four possible limitations in the model for C_4 photosynthesis.

Gas exchange measurements of photosynthetic CO_2-response curves have been widely used to estimate parameters of the FvCB model (Dubois et al., 2007; Sharkey et al., 2007). Combined gas exchange and chlorophyll fluorescence measurements have also been used to estimate additional photosynthetic parameters, such as mesophyll conductance (g_m) (Evans and von Caemmerer, 1996), utilizing the fact that photosystem II (PSII) e^- transport efficiency could be assessed by chlorophyll fluorescence measurement (Genty et al., 1989). Using combined gas exchange and chlorophyll fluorescence measurements of both CO_2- and light-response curves, Yin et al. (2009) and Yin et al. (2011b) described methods to estimate photosynthetic parameters for C_3 and C_4 photosynthesis, respectively. There are many reports on using these methods to estimate photosynthetic parameters within an individual species. However, estimating these photosynthetic parameters simultaneously for major C_3 and C_4 crops to better support yield forecasting of these crops is rare.

Key photosynthetic parameters such as V_{cmax} and J_{max} are known to correlate with leaf N content (LNC) (Evans and Clarke, 2019; Harley et al., 1992b; Niinemets and Tenhunen, 1997). This is because N is a key-element in various photosynthetic machineries, such as the light harvesting complexes, the e^- transport systems, the CO_2 fixation enzymes, and other enzymes (Laisk et al., 2002). Within chloroplasts, 84% of N is associated with photosynthesis-related proteins and molecules and 75% of N in mature leaves is present in chloroplasts (Evans and Clarke, 2019).

In this study, photosynthetic parameters of the FvCB models will be estimated by combined gas exchange and chlorophyll fluorescence measurements for four major crops (C_3: rice and wheat, C_4: maize and sorghum) under three different N levels. Our objectives are: 1) to quantify photosynthetic parameters for these C_3 and C_4 crop species; 2) to quantify the relationships of these parameters with LNC; and 3) to assess if these relationships differ between different crop species. These relationships are discussed in the context of crop modelling in order to better support N management in smart production of major crops.

2. Materials and methods

2.1. Plant materials and growth conditions

The experiment was conducted as a split-plot design (crop species as the whole-plot factor, N treatment as the split-plot factor), with four replicates. The selected C_3 crops were rice (cv. IR64) and wheat (cv. Paragon), and the C_4 crops were maize (cv. P8057) and sorghum (cv. CSM63E). Seeds were sown in 7-L pots with 5.2 L soil. Soil was prepared by mixing sandy soil and perlite substrate in equal volumes for wheat, maize and sorghum while for rice, perlite substrate was substituted by quartz sand. Plants were grown under well-watered conditions in a greenhouse of UNIFARM, Wageningen University & Research, the Netherlands. Natural light was automatically supplemented by an artificial light source (600 W HPS Hortilux Schréder Lamps, Monster, Netherlands), which was switched on when global solar radiation outside the greenhouse dropped below 400 W m^{-2} and switched off when it exceeded 500 W m^{-2}. The photoperiod was 12 h d^{-1}. The average temperature was 25–27 °C during the day and 22–23 °C during the night, and the relative humidity was 60–80%. Nitrogen was supplied weekly through a nutrient solution and three N levels (low N: 50 mg N; middle N: 300 mg N; and high N: 1000 mg N, per pot) were applied resulting in

three different LNC levels. Seeds were sown for four consecutive weeks to create four replicates of plants so that the workload for measurements (see below) could be spread over weeks; one leaf was tagged per replicate for conducting measurements.

2.2. Gas exchange and chlorophyll fluorescence measurements

Measurements were conducted on selected leaves (the 6–8th for rice, the 6–7th for wheat, the 5th for maize and the 7–8th for sorghum, counted from below), on average 9 days after full expansion of the leaves. Simultaneous gas exchange and chlorophyll fluorescence measurements were conducted over the same leaf area, using an open gas exchange system Li-Cor 6400XT and an integrated fluorescence chamber head (Li-Cor, Lincoln, Nebraska, USA). During the measurements, the leaf temperature was set at 25 °C and the leaf-to-air vapour pressure difference was controlled within a range of 0.6–1.9 kPa.

First, incident irradiance (I_{inc}) response curves of net photosynthetic rate (A) at the 21% O_2 level were assessed. Photon flux density (at a red:blue ratio of 90%:10%) was decreased stepwise: 1750, 1000, 500, 200, 150, 100, 70, and 45 μmol m^{-2} s^{-1} while keeping ambient CO_2 (C_a) at 400 μmol mol^{-1}. To obtain a CO_2 response curve of A at 21% O_2, C_a was first decreased stepwise: 400, 250, 150, 100, and 65 μmol mol^{-1} and then increased stepwise: 400, 600, 1000, and 1500 μmol mol^{-1} while keeping I_{inc} at a saturating level, 1750 μmol m^{-2} s^{-1}, evidenced by the above observed I_{inc} response curves at the 21% O_2 level. In order to convert chlorophyll fluorescence-based apparent PSII photochemical efficiency into linear e^- transport for C_3 crops and into ATP production rate for C_4 crops (see below), an extra I_{inc} response curve was measured, in which photon flux densities were in a decreasing series: 350, 200, 150, 100, 70, and 45 μmol m^{-2} s^{-1} while keeping C_a at 1000 μmol mol^{-1} combined with 2% O_2 to ensure a non-photorespiratory condition. All gas exchange data were measured at a constant flow rate (300 μmol s^{-1}).

At each step in I_{inc} or C_a, the steady-state fluorescence yield (F_s) was recorded once A reached the steady state (taking 5 min on average to reach). Afterwards, the multiphase flash was applied to estimate the maximum fluorescence yield (F_m') (Loriaux et al., 2013). The photon flux density was increased from 2500 to ca 8450 μmol m^{-2} s^{-1} (Phase 1), then attenuated by 40% (Phase 2) and finally increased back to 8450 μmol m^{-2} s^{-1} (Phase 3). F_m' was estimated as the intercept of the linear regression of fluorescence yield in Phase 2 against the reciprocal of flash intensity. The apparent quantum efficiency of PSII e^- transport (Φ_2) was calculated as $\Delta F/F_m' = (F_m' - F_s)/F_m'$ (Genty et al., 1989).

All gas exchange data and the CO_2 level of the substomatal cavity (C_i) were corrected for CO_2 leakage in the chamber based on apparent CO_2 response curves using heat-killed leaves (Flexas et al., 2007), measured with the same flow rate (300 μmol s^{-1}).

2.3. Leaf N content assessment

A leaf portion from the leaf position used for measuring photosynthesis was excised for N content measurements. For rice and wheat, a 5-6-cm long part of a leaf was cut down to measure specific leaf area. For maize and sorghum, a 2-cm^2 leaf disk was punched. All leaf materials were weighed after drying at 70 °C to constant weight. Then, total N concentration was analyzed using the Micro-Dumas combustion method. Leaf N content on the area basis (LNC) was derived from these data.

2.4. C_3 model

The calculation of A_c and A_j in the FvCB model is proposed as (Farquhar et al., 1980):

$$A = \frac{(C_c - \Gamma_*)x_1}{C_c + x_2} - R_d \quad (1)$$

where for A_c, $x_1 = V_{cmax}$ and $x_2 = K_{mC}(1 + O_c/K_{mO})$; for A_j, $x_1 = J/4$ and $x_2 = 2\Gamma^*$. In the model, C_c is the CO_2 level at the carboxylation site of Rubisco and Γ^* is the CO_2 compensation point in the absence of day respiration (R_d), defined as $0.5O_c/S_{c/o}$, where O_c is the O_2 level in chloroplasts and $S_{c/o}$ is the relative CO_2/O_2 specificity factor for Rubisco (von Caemmerer et al., 1994). K_{mC} and K_{mO} are Michaelis-Menten constants of Rubisco for CO_2 and O_2, respectively (Table 1). J is the linear e^- transport rate.

If the TPU limitation occurs, A can be simplified as

$$A_p = 3T_p - R_d \quad (2)$$

Overall, the C_3 model predicts A as the minimum of three limited rates of CO_2 assimilation:

$$A = min(A_c, A_j, A_p) \quad (3)$$

Eqn (1) uses C_c as input, but C_c is generally unknown. This is commonly solved by combining Eqn (1) and the Fick's law of gas diffusion $C_c = C_i - A/g_m$, and the obtained solution for A can be expressed as a quadratic function of C_i (von Caemmerer, 2000). This procedure assumes that the mesophyll conductance g_m is constant (i.e. independent of light or CO_2 levels at the given temperature) based on early reports (e.g. Loreto et al., 1992). However, our result based on the variable J method of Harley et al. (1992a) showed that g_m was variable, varying with C_i and light levels (see Results). Thus, we used a simplified version of the model (Yin et al., 2009), in which a dimensionless parameter δ is introduced dealing with variable g_m (see Appendix A) in such a way that g_m values at various C_i and light levels are emergent properties of the parameter δ (see later).

2.5. C_4 model

For C_4 species, A is written as (von Caemmerer and Furbank, 1999):

$$A = V_p - L - R_m \quad (4)$$

where V_p is the rate of PEP carboxylation in the mesophyll cells, L is the CO_2 leakage rate from the bundle sheath to the mesophyll, and R_m is the

Table 1
Pre-set model parameters with their definitions and values.

Parameter	Definition	C_3 species		C_4 species	
		Value	Reference	Value	Reference
K_{mC}	Michaelis-Menten constant of Rubisco for CO_2 (μmol mol^{-1})	291	Cousins et al. (2010)	485	Cousins et al. (2010)
K_{mO}	Michaelis-Menten constant of Rubisco for O_2 (mmol mol^{-1})	194	Cousins et al. (2010)	146	Cousins et al. (2010)
K_P	Michaelis-Menten constant of PEPc for CO_2 (μmol mol^{-1})	–		40	Leegood and von Caemmerer (1989)
$S_{c/o}$	Relative CO_2/O_2 specificity of Rubisco (mmol $\mu$$mol^{-1}$)	3.022	Cousins et al. (2010)	2.862	Cousins et al. (2010)
α	Fraction of O_2 evolution in bundle sheath cells (–)	–		0.1	Chapman et al. (1980)
x	Fraction of ATP used for CCM (–)	–		0.4	von Caemmerer and Furbank (1999)
n_b	Base leaf nitrogen, at and below which leaf photosynthesis is zero (g N m^{-2})	–		0.24	Yin et al. (2011b)

mitochondrial respiration rate occurring in mesophyll cells, considered as $R_d/2$ (von Caemmerer and Furbank, 1999), where R_d is leaf day respiration, the same as defined for the C_3 model.

The standard C_4 model assumes that C_4 acid decarboxylation in bundle sheath cells is not limited and occurs at the same rate as V_p. If V_p is PEP carboxylase limited, V_p is described as:

$$V_p = \frac{C_m V_{pmax}}{C_m + K_p} \tag{5a}$$

where V_{pmax} is the carboxylation capacity of PEPc; K_p is the Michaelis-Menten constant of PEPc for CO_2; C_m is the CO_2 concentration of mesophyll cells, described as $C_m = C_i - A/g_m$, following the Fick's law of gas diffusion. So far, there is no strong evidence reported for variable g_m in C_4 species; so, we treated g_m as a constant, in contrast with the C_3 case. If V_p is e^- transport limited, V_p is expressed as:

$$V_p = xJ_{atp}/2 \tag{5b}$$

where x is the partition fraction of ATP to the C_4 cycle and J_{atp} is the ATP production rate driven by e^- transport. Note that the constant 2 in eqn (5b) applies to the C_4 subtype to which maize and sorghum belong; this coefficient may need to change if the model is applied to other subtypes (Yin et al., 2021a).

The term L in eqn (4) is given by:

$$L = g_{bs}(C_c - C_m) \tag{6}$$

in which g_{bs} is the bundle sheath conductance and C_c is the CO_2 concentration at the carboxylation site of Rubisco in bundle sheath cells.

As for the Rubisco carboxylation and oxygenation reactions in the bundle sheath cells, A can be written, like in the C_3 photosynthetic model, as:

$$A = \frac{(C_c - \gamma_* O_c)x_1}{C_c + x_2 O_c + x_3} - R_d \tag{7}$$

where γ^* is defined as $0.5/S_{c/o}$, O_c is the O_2 level at the carboxylation sites of Rubisco in the bundle sheath cells, described as $O_c = \alpha A/(0.047 g_{bs}) + O_i$, where α is the fraction of O_2 evolution happening in bundle sheath cells (von Caemmerer and Furbank, 1999). When enzymatic activity limits, $x_1 = V_{cmax}$, $x_2 = K_{mC}/K_{mO}$ and $x_3 = K_{mC}$. When A is limited by e^- transport, $x_1 = (1 - x)J_{atp}/3$, $x_2 = 7\gamma^*/3$ and $x_3 = 0$ (Yin et al., 2011b).

Consequently, as the reactions related to both C_3 and C_4 cycles can be limited by either enzyme activity or e^- transport, the four-limitation C_4 model is described as:

$$A = min(A_{EE}, A_{ET}, A_{TE}, A_{TT}) \tag{8}$$

where A_{EE} represents A when both C_3 and C_4 cycles are limited by enzyme actions, A_{ET} is A when the C_4 cycle is limited enzymatically and the C_3 cycle is limited by e^- transport, A_{TE} is A when the C_4 cycle is limited by e^- transport and the C_3 cycle is limited enzymatically, and A_{TT} means A when both cycles are limited by e^- transport. Mathematical solutions to A_{EE}, A_{ET}, A_{TE}, and A_{TT} are from Yin et al. (2011b) and are given in Appendix B.

2.6. Estimation steps of model parameters

The procedures of Yin et al. (2009) and Yin et al. (2011b) are adopted to estimate C_3 and C_4 photosynthetic parameters, respectively.

2.6.1. Estimating calibration factor (s) and day respiration (R_d)

To convert chlorophyll fluorescence-based data for PSII e^- transport efficiency into linear e^- transport rate J (C_3) or to ATP production rate J_{atp} (C_4) as required by their respective models (see Eqn (1) and Eqn (7)), it is necessary to obtain a calibration factor based on measurements under non-photorespiratory condition (Bernacchi et al., 2003; Valentini et al., 1995). We followed the procedure of Yin et al. (2009) and Yin et al. (2011b) for C_3 and C_4 models, respectively, for this calibration. Unlike other calibration methods, their procedure simultaneously provides an estimate of R_d, because the calibration factor s and day respiration R_d were estimated as the slope and intercept, respectively, of the linear regression of A against $I_{inc}\Phi_2/4$ for C_3 species (Yin et al., 2009) and of A against $I_{inc}\Phi_2/3$ for C_4 species (Yin et al., 2011b), using data under the non-photorespiratory condition. Different stoichiometric coefficients (4 vs 3) were used to agree with the A_j submodel, which was formulated in terms of e^- and ATP demands by the C_3 cycle for C_3 and C_4 models, respectively (see the e^- transport limited part of Eqn (1) and Eqn (7)). To distinguish them, the slope factor was denoted as s_{c3} and s_{c4} for C_3 and C_4 species, respectively. The selected data for this linear regression was from combined measurements of gas exchange and chlorophyll fluorescence within the e^- transport-limited range (i.e. with I_{inc} between 20 and 200 μmol m^{-2} s^{-1}) under non-photorespiratory conditions (keeping C_a at 1000 μmol mol^{-1} combined with 2% O_2, which is supposed to suppress photorespiration).

2.6.2. Estimating PSII electron transport efficiency under limiting light (Φ_{2LL})

Φ_{2LL} was estimated by fitting the light response curve of Φ_2 to the equation (Yin et al., 2009):

$$\Phi_2 = \left[\alpha_{2LL} I_{inc}\beta + J_{2max} - \sqrt{(\alpha_{2LL} I_{inc}\beta + J_{2max})^2 - 4\theta_2 J_{2max}\alpha_{2LL} I_{inc}\beta}\right] \Big/ (2\theta_2 \alpha_{2LL} I_{inc}\beta/\Phi_{2LL}) \tag{9}$$

where α_{2LL} is the quantum efficiency of PSII e^- transport under limiting light on the combined PSI- and PSII-absorbed light basis and given as $\Phi_{2LL}(1 - f_{cyc})/[\Phi_{2LL}/\Phi_{1LL} + (1 - f_{cyc})]$, in which f_{cyc} is the fraction of e^- at PSI that follow cyclic e^- transport around PSI and Φ_{1LL} is the quantum efficiency of PSI e^- transport under limiting light on the PSI-absorbed light basis. β is the leaf absorptance by photosynthetic pigments, J_{2max} is the maximum rate of all e^- transport through PSII under saturated light (J_2) and θ_2 is the convexity factor for response of J_2 to absorbed photon flux density (I_{abs}). Since θ_2 and Φ_{2LL} are not affected by the various values of f_{cyc} or Φ_{1LL}, arbitrary yet physiologically relevant values of f_{cyc} (e.g. 0) or Φ_{1LL} (e.g. 1.0) can be used to estimated Φ_{2LL} (Yin et al., 2009). Thus, with measured I_{inc}, β and Φ_2, Φ_{2LL}, θ_2 and J_{2max} can be fitted as output. As estimated θ_2 and J_{2max} are not used in the FvCB model, only Φ_{2LL} will be discussed later.

2.6.3. Calculating electron transport parameters

Once s and Φ_{2LL} are known, for C_3 species, the efficiency of converting incident irradiance into linear e^- transport (κ_{2LL}) can be calculated as $s_{c3}\Phi_{2LL}$ (Yin et al., 2009). Following a standard model, the light response curve of the calculated J can be described by:

$$C_3: \quad J = \left[\kappa_{2LL} I_{inc} + J_{max} - \sqrt{(\kappa_{2LL} I_{inc} + J_{max})^2 - 4\theta J_{max}\kappa_{2LL} I_{inc}}\right] \Big/ (2\theta) \tag{10a}$$

where J_{max} is the light-saturated maximum value of linear e^- transport rate, and θ is a curvature factor. Values of J_{max} and θ can be estimated by fitting eqn (10a) to the data for the light response curve of the calculated J ($= s_{c3} I_{inc}\Phi_2$).

Compared with C_3 species, energy supply is more complex in C_4 species because of the coordinated functioning of mesophyll and bundle sheath cells. Nonetheless, as energy is highly likely to be shared between the two types of cells (Kanai and Edwards, 1999), modelling energy

supply or production rate as a whole is pragmatic and sufficient for our analysis on the basis of measurements of photosynthetic quantum yield and PSII photochemical efficiency conducted on the whole leaf (von Caemmerer and Furbank, 1999; Yin and Struik, 2012). This is achieved using a factor, x, for energy partitioning to the C_4 cycle, and $(1 - x)$ for partitioning to the C_3 cycle (see eqn (5b) and eqn (7), respectively). Thus, for C_4 species, J_{atp} can be calculated as $J_{atp} = s_{c4}I_{inc}\Phi_2/(1 - x)$ (Yin et al., 2011b). Alike with Eqn (10a), the light response curve of J_{atp} can be described as (Yin et al., 2011b):

$$C_4 : J_{atp} = \left[\kappa_{2LL,atp}I_{inc} + J_{max,atp} - \sqrt{\left(\kappa_{2LL,atp}I_{inc} + J_{max,atp}\right)^2 - 4\theta J_{max,atp}\kappa_{2LL,atp}I_{inc}}\right] \Big/ (2\theta) \quad (10b)$$

where $\kappa_{2LL,atp}$, the efficiency of converting incident light into ATP under limiting light, was calculated by $s_{c4}\Phi_{2LL}/(1 - x)$. Thus, the light-saturated maximum value of ATP production rate, $J_{max,atp}$, can be estimated from fitting Eqn (10b) to the light response curve of the calculated J_{atp}.

2.6.4. Estimating T_p and δ

Since prediction of A_c is affected by possible uncertainties of K_{mC} and K_{mO} (see sensitivity analysis later), g_m was estimated after embedding $J = s_{c3}I_{inc}\Phi_2$ into the A_j model (see eqns A1 and A2 in Appendix A) for C_3 species (Yin et al., 2009). Hence, the parameter δ in the g_m model and T_p were parameterized together using measured data under limiting light ($I_{inc} < 200$ μmol m^{-2} s^{-1}) of the A-I_{inc} curves and higher ambient CO_2 ($C_a > 400$ μmol mol^{-1}) of the A-C_i curves where A is expected to be limited either by e^- transport or by TPU.

2.6.5. Estimating V_{cmax} and other parameters

In our study, in order to have a better fit of measured data, J_{max} and θ for C_3 species were estimated together with V_{cmax} by fitting the complete C_3 model (see Appendix A) combined with Eqn (10a) based on the whole dataset, using estimated R_d, κ_{2LL}, δ and T_p as input. As J_{max} differed between non-photorespiratory and photorespiratory conditions, the dummy variable method (Yin et al., 2009) was used for the different values of J_{max} under 21% and 2% O_2 conditions.

For C_4 species, with estimated R_d and s_{c4} as input, the complete C_4 model (see Appendix B) combined with $J_{atp} = s_{c4}I_{inc}\Phi_2/(1 - x)$ was used for estimating g_{bs}, V_{cmax} and V_{pmax} simultaneously from fitting to the whole dataset. As g_m is less important than g_{bs} in C_4 species, in order to reduce over-fitting, an overall estimate for g_m was made and g_{bs} was estimated based on the proven linear relationship between g_{bs} and (LNC – n_b), where n_b is the base leaf N, at which leaf photosynthesis reduces to zero (Retta et al., 2016; Yin et al., 2011b).

2.6.6. Calculating the dependence of g_m in C_3 species in response to C_i and I_{inc}

Once all parameters were obtained, the dependence of g_m on light and CO_2 in C_3 species was back-calculated based on the following equation by Yin et al. (2009):

$$g_m = A + \delta(A + R_d)/(C_i - \Gamma_*) \quad (11)$$

where A is modelled net CO_2 assimilation rate for specific light and CO_2 levels.

2.7. Model input constants and statistical analyses

As many parameters of the FvCB model and its C_4 equivalents are conserved, we set these conserved parameters to constant values (Table 1). The definitions of estimated model parameters are listed in Table 2.

Simple linear regression was carried out by Microsoft Excel. Non-linear regression was performed in SAS using the GAUSS method in PROC NLIN (SAS Institute Inc, Cary, NC, USA). Data for individual replicates were pooled to obtain robust parameter estimates for each treatment.

The difference between C_3 and C_4 species in LNC was evaluated by the use of the Student's t-test in Excel. Photosynthetic parameters were linearly regressed against LNC, for which only the estimates of the parameter for N treatments were used. Analysis of covariance (ANCOVA) was conducted in R (R Core Team, 2021) to examine any significant differences in the regression equations between crops.

Table 2
Model parameters to be estimated.

Parameter	Definition
g_{bs}	Bundle sheath diffusion conductance (mol m^{-2} s^{-1})
g_m	Mesophyll diffusion conductance (mol m^{-2} s^{-1})
J_{max}	Maximum rate of linear e^- transport for C_3 species under saturated light (μmol e^- m^{-2} s^{-1})
$J_{max,atp}$	Maximum chloroplastic ATP production rate for C_4 species under saturated light (μmol ATP m^{-2} s^{-1})
R_d	Day respiration (μmol CO_2 m^{-2} s^{-1})
s_{c3}	A lumped parameter as the calibration factor for C_3 species (mol CO_2 (mol CO_2)$^{-1}$)
s_{c4}	A lumped parameter used to estimate R_d for C_4 species (mol ATP (mol e^-)$^{-1}$)
T_p	Rate of triose phosphate export from the chloroplast (μmol phosphate m^{-2} s^{-1})
V_{cmax}	Maximum rate of Rubisco activity-limited carboxylation (μmol CO_2 m^{-2} s^{-1})
V_{pmax}	Maximum rate of PEPC activity-limited carboxylation (μmol CO_2 m^{-2} s^{-1})
χ_{gbs}	Linear slope of bundle-sheath conductance versus (LNC – n_b) (mmol CO_2 g^{-1} N s^{-1})
χ_{Jmax}	Linear slope of J_{max} versus LNC (μmol e^- g^{-1} N s^{-1})
$\chi_{Jmax,atp}$	Linear slope of $J_{max,atp}$ versus LNC (μmol ATP g^{-1} N s^{-1})
χ_{Tp}	Linear slope of T_p versus LNC (μmol phosphate g^{-1} N s^{-1})
χ_{Vcmax}	Linear slope of V_{cmax} versus LNC (μmol CO_2 g^{-1} N s^{-1})
χ_{Vpmax}	Linear slope of V_{pmax} versus LNC (μmol CO_2 g^{-1} N s^{-1})
δ	Parameter to quantify the variable g_m, representing the carboxylation to mesophyll resistance ratio (–)
κ_{2LL}	Conversion efficiency of incident light into linear e^- transport for C_3 species at the strictly limiting light level (mol e^- (mol photon)$^{-1}$)
$\kappa_{2LL,atp}$	Conversion efficiency of incident light into ATP production for C_4 species at the strictly limiting light level (mol ATP (mol photon)$^{-1}$)
Θ	Convexity factor for response of e^- transport or of ATP production to incident light (–)
Φ_{2LL}	Φ_2 at the strictly limiting light level (mol mol^{-1})

3. Results

3.1. Effects of N supply on photosynthetic capacity A_{max}

Measured A while keeping incident I_{inc} at 1750 μmol m^{-2} s^{-1} and C_a at 400 μmol mol^{-1} in A-I_{inc} curves were recorded as A_{max}. When O_2 level decreased from 21% to 2%, A_{max} increased in rice and wheat due to suppressed photorespiration; but this increase was very small in maize and sorghum as a result of the operation of CCM in C_4 species (Fig. 1). Under the same leaf N conditions, A_{max} of maize was higher than that of sorghum and there was a significant difference in the intercept of their regression equations for the A_{max}-LNC linear plot ($p < 0.05$). Moreover, the linear regression equation of A_{max} versus LNC for C_4 species differed significantly from that for C_3 species under both O_2 conditions in terms of either slope or intercept ($p < 0.05$) (Table S1). The increasing trends of A_{max} of rice and wheat were similar when LNC ranged from 0.59 to 1.44 g N m^{-2}, but LNC of wheat plants of the high-N treatment reached 2.21 g N m^{-2} and A_{max} at this high LNC tended to level off (Fig. 1a).

3.2. Estimations of calibration factor and day respiration R_d

Calibration factor and R_d were estimated by linear regression (Fig. 2). Estimated values of s_{c3} were in the range of 0.455–0.582 mol CO_2 (mol

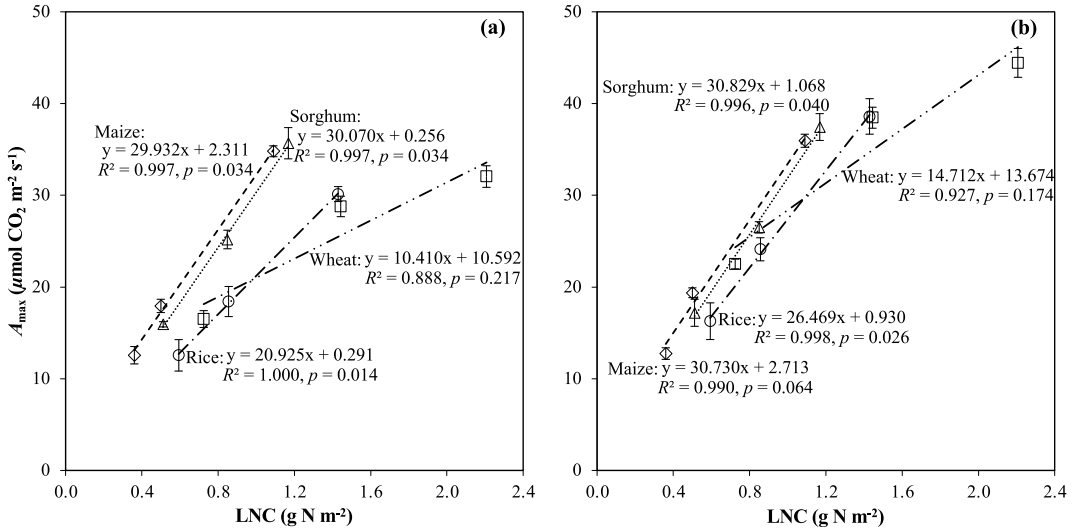

Fig. 1. Measured A_{max} (maximum rate of light saturated assimilation at ambient CO_2 level) in relation to LNC (leaf nitrogen content) for rice (circles), wheat (squares), maize (diamonds) and sorghum (triangles) under conditions of 21% (a) and 2% O_2 (b). Data points are shown with bars for standard errors of the means.

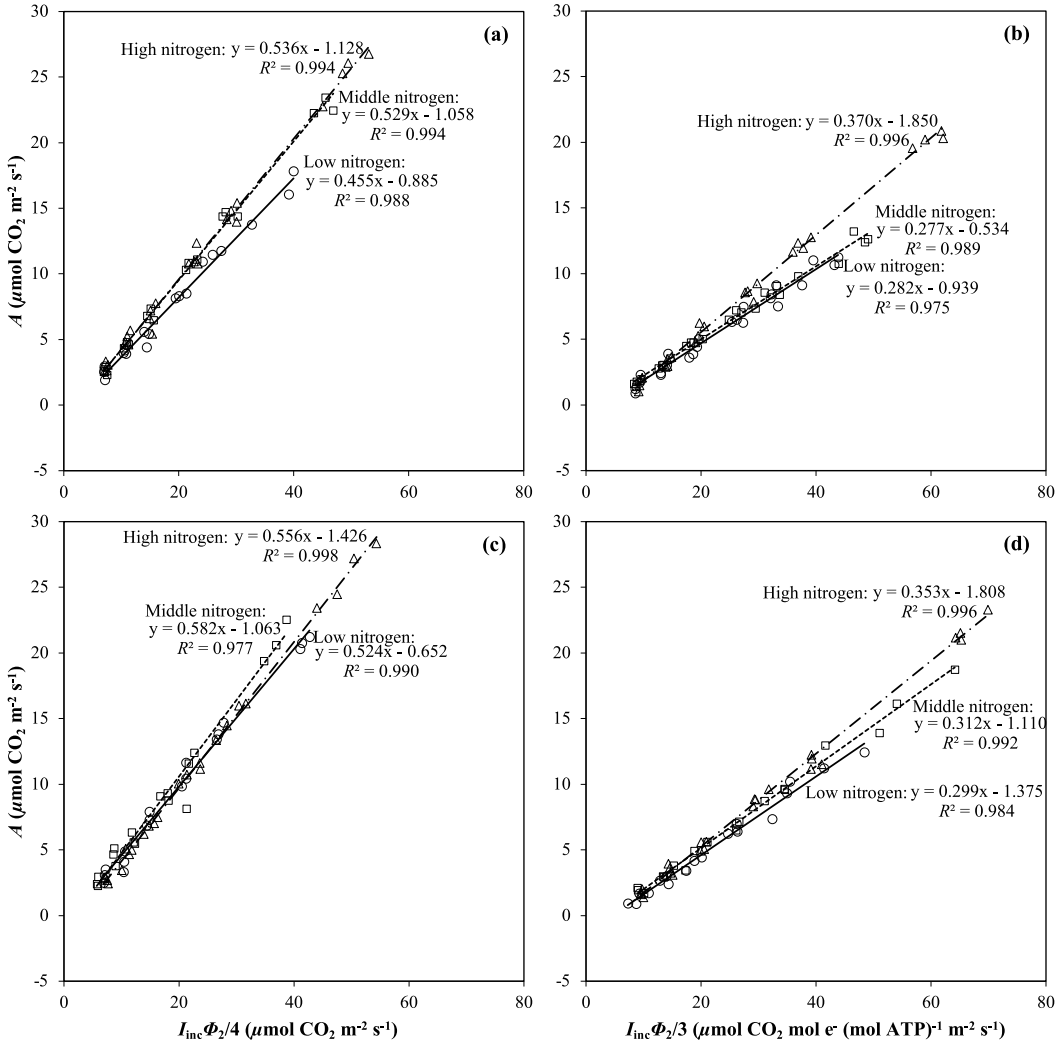

Fig. 2. Linear regression of assimilation rate A against $I_{inc}\Phi_2/4$ of rice (a), wheat (c), and of A against $I_{inc}\Phi_2/3$ of maize (b) and sorghum (d) under low- (open circles), middle- (open squares), and high- (open triangles) nitrogen supply, respectively. Measurements were conducted under non-photorespiratory condition. Each data point reflects measurement of individual replicate. The intercept of the regression represents the estimation of day respiration (R_d), and the slope represents the estimation of the calibration factor (i.e. s_{c3} for rice and wheat, and s_{c4} for maize and sorghum; see the text).

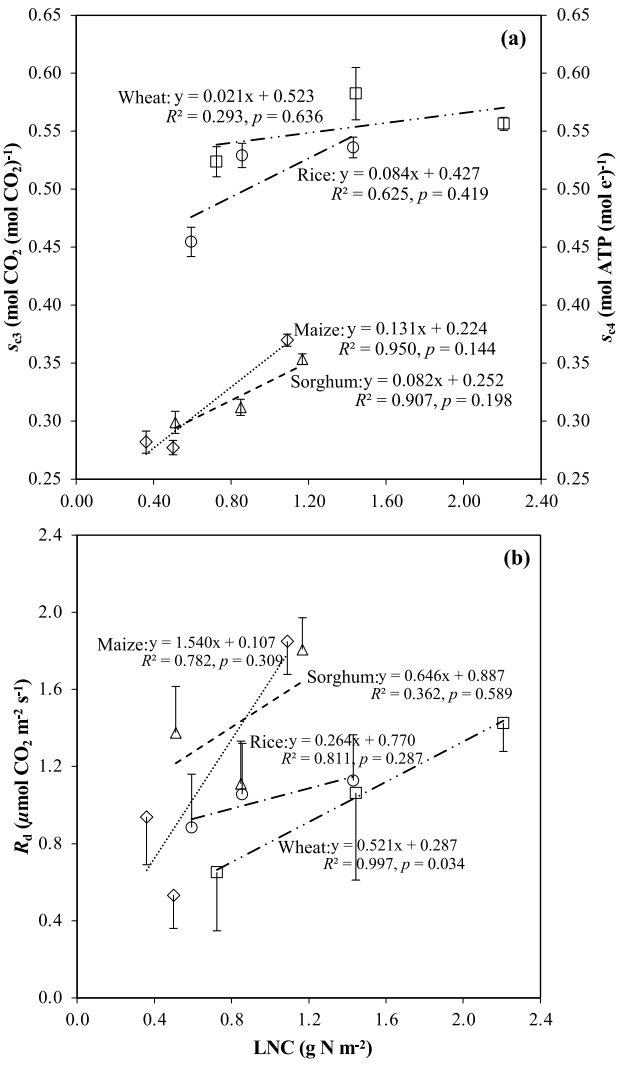

Fig. 3. Calibration factor for C_3 crops s_{c3} or for C_4 crops s_{c4} (a) and day respiration R_d (b) in relation to leaf nitrogen content (LNC). Rice (circles), wheat (squares), maize (diamonds) and sorghum (triangles). The vertical bars represent the standard errors of the estimates.

$CO_2)^{-1}$ and s_{c4} varied from 0.277 to 0.370 mol ATP (mol e^-)$^{-1}$. The linear relationship between s_{c3} of C_3 crops and LNC was non-significant ($p > 0.05$) (Fig. 3a). Likewise, s_{c4} increased with LNC for C_4 crops, but non-significantly ($p > 0.05$) (Fig. 3a). The estimated R_d increased with LNC, but non-significantly in both C_3 and C_4 crops ($p > 0.05$) (Fig. 3b). Moreover, there was no significant ($p > 0.05$) difference in these regressed linear equations between rice and wheat, nor between maize and sorghum.

3.3. Estimations of photosynthetic efficiency parameters

Estimated Φ_{2LL} ranged from 0.49 to 0.70 mol mol^{-1} and was higher in C_3 species than in C_4 species under both 21% and 2% O_2 levels (Table 3). The increase of Φ_{2LL} with LNC for both C_3 and C_4 species was non-significant ($p > 0.05$) under any of the two O_2 levels (Table S1). Φ_{2LL} changed slightly with increasing O_2 level from 2% to 21% and the ratio of estimated value of Φ_{2LL} under 21% and 2% O_2 levels varied from 1.02 to 1.07 among the four species.

The estimated κ_{2LL} values of the C_3 species were in the range of 0.285–0.389 mol e^- (mol photon)$^{-1}$ and $\kappa_{2LL,atp}$ of C_4 species varied from 0.254 to 0.382 mol ATP (mol photon)$^{-1}$. As κ_{2LL} and $\kappa_{2LL,atp}$ were calculated from calibration factor (s_{c3} and s_{c4}) and Φ_{2LL} (which both varied slightly with LNC), it follows that κ_{2LL} and $\kappa_{2LL,atp}$ increased with increasing LNC (Table 3).

3.4. Estimation of CO_2-diffusion parameters

For rice and wheat, we first calculated g_m using the commonly used method of Harley et al. (1992a), which showed that g_m varied with C_i and I_{inc} and was zero at the zero irradiance (Fig. S1). We thus incorporated the variable-g_m formula into the FvCB equation for A_j to estimate the parameter δ (see Appendix A). The calculated g_m at A_{max} from using this variable-g_m algorithm, i.e. eqn (11), had a good linear relationship with LNC as well (Fig. 4a). If LNC was at the same level, g_m of rice tended to be higher than g_m of wheat (Fig. 4a).

With respect to C_4 species, we were not able to judge whether or not CO_2-diffusion parameters are variable, so an overall g_m was estimated from fitting the C_4 model (Appendix B) to measurements. The estimated g_m was 2.99 (s.e. 0.65) and 1.87 (s.e. 0.28) mol m^{-2} s^{-1} for maize and sorghum, respectively, which were - not surprisingly - higher than the values of the C_3 species. g_{bs} was estimated under different N supplies and both the estimated g_{bs} and its response slope to LNC were lower in maize than in sorghum (Fig. 4b).

3.5. Estimations of photosynthetic capacity parameters and their linear slopes with LNC

There were significant and positive linear relationships between estimated photosynthetic capacity parameters and LNC (Table S1). Within C_3 species, the regression slope of J_{max} versus LNC (χ_{Jmax}) of rice was significantly ($p < 0.05$) higher than that of wheat, while the difference of the intercept was non-significant ($p > 0.05$), as reflected by the higher values of estimated J_{max} of wheat than rice under low N input but

Table 3
Estimated (standard error in brackets if applicable) of Φ_{2LL} and κ_{2LL} or $\kappa_{2LL,atp}$. Estimates are made separately for different O_2 conditions.

Parameter		Low nitrogen	Mid nitrogen	High nitrogen	Low nitrogen	Mid nitrogen	High nitrogen
		Rice			Wheat		
LNC (g N m^{-2})		0.593 (0.032)	0.856 (0.038)	1.429 (0.068)	0.724 (0.054)	1.444 (0.115)	2.208 (0.068)
Φ_{2LL} (mol mol^{-1})	21% O_2	0.645 (0.026)	0.681 (0.010)	0.683 (0.006)	0.618 (0.025)	0.631 (0.012)	0.699 (0.013)
	2% O_2	0.626 (0.040)	0.671 (0.015)	0.669 (0.009)	0.557 (0.021)	0.601 (0.018)	0.660 (0.013)
κ_{2LL}[a] [mol e^- (mol photon)$^{-1}$]	21% O_2	0.293	0.360	0.366	0.323	0.367	0.389
	2% O_2	0.285	0.355	0.359	0.292	0.350	0.367
		Maize			Sorghum		
LNC (g N m^{-2})		0.361 (0.018)	0.500 (0.051)	1.090 (0.068)	0.511 (0.042)	0.849 (0.063)	1.168 (0.055)
Φ_{2LL} (mol mol^{-1})	21% O_2	0.593 (0.016)	0.605 (0.007)	0.601 (0.003)	0.594 (0.023)	0.531 (0.007)	0.649 (0.016)
	2% O_2	0.581 (0.019)	0.591 (0.009)	0.586 (0.005)	0.565 (0.018)	0.489 (0.008)	0.618 (0.020)
$\kappa_{2LL,atp}$[a] [mol ATP (mol photon)$^{-1}$]	21% O_2	0.279	0.279	0.371	0.296	0.276	0.382
	2% O_2	0.273	0.273	0.362	0.282	0.254	0.364

[a] Since κ_{2LL} and $\kappa_{2LL,atp}$ were calculated as $s_{c3}\Phi_{2LL}$ and $s_{c4}\Phi_{2LL}/(1-x)$ (see materials and methods) for C_3 and C_4 crops, respectively, standard errors are not available for these variables.

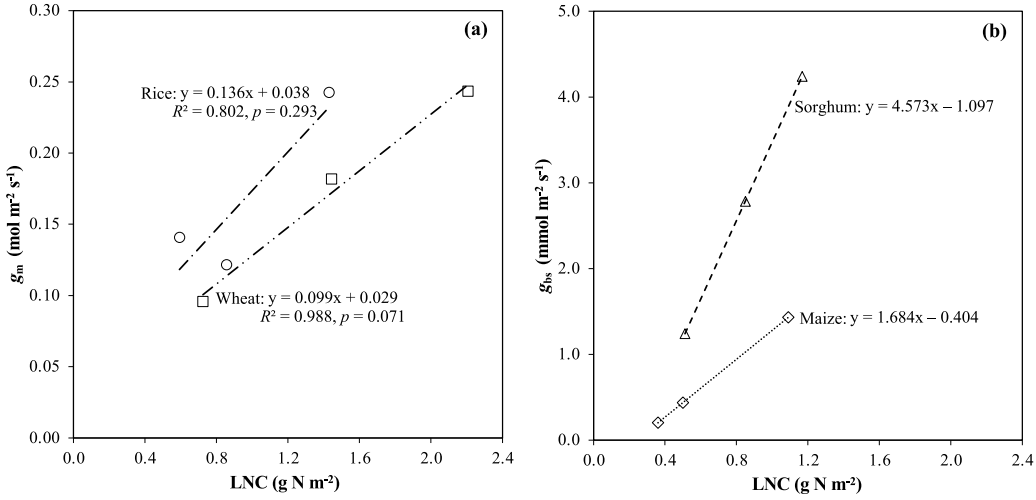

Fig. 4. Mesophyll conductance g_m (a) of rice (circles) and wheat (squares) and bundle-sheath conductance g_{bs} (b) of maize (diamonds) and sorghum (triangles) in relation to leaf nitrogen content (LNC). In Panel a, g_m represents the value of g_m when A reached A_{max} (i.e. keeping I_{inc} at 1750 μmol m^{-2} s^{-1} and C_a at 400 μmol mol^{-1}). The estimated g_{bs} of maize and sorghum were calculated from the equation, $g_{bs} = \chi_{gbs}(LNC - n_b)$, where the linear slope χ_{gbs} was estimated, together with other parameters, from fitting the full C_4 model to the whole data of each crop (see the text); thus, there are no R^2 and p values for the equations in Panel b.

lower values for wheat under high N input (Fig. 5a). For the C_4 crops, $J_{max,atp}$ of maize was higher than that of sorghum, although there was no significant difference ($p > 0.05$) between regressed linear equations of $J_{max,atp}$ versus LNC in both crops.

The estimate of V_{cmax} increased with LNC in both C_3 and C_4 species (Fig. 5b) and the equation of V_{cmax} versus LNC for C_3 species was significantly ($p < 0.01$) different from that for C_4 species in the intercept, but not in the slope (χ_{Vcmax}) ($p > 0.05$). Moreover, χ_{Vcmax} of rice was significantly ($p < 0.05$) higher than that of wheat. However, the response of V_{cmax} to LNC was weak in C_4 species and there was no significant ($p > 0.05$) difference between maize and sorghum (Fig. 5b).

The estimate of T_p in C_3 species (Fig. 5c) and that of V_{pmax} in C_4 species (Fig. 5d) increased with LNC. But the trend of T_p with LNC did not differ significantly ($p > 0.05$) between rice and wheat, nor did that of V_{pmax} with LNC between maize and sorghum.

Together with above mentioned photosynthetic capacity parameters in C_3 and C_4 species, the convexity factor θ was estimated. The overall estimated θ was 0.84 (0.02) and 0.81 (0.02) for rice and wheat, respectively, while its value was up to 0.98 (0.01) and 0.99 (0.01) for maize and sorghum, respectively (results not shown).

3.6. Modelled CO_2 and irradiance responses of net assimilation rate

The modelled versus measured A-C_i and A-I_{inc} curves across crop species × N supply combinations are shown in Fig. S2. A increased with N supply and such an effect tended to be enlarged when suppressing O_2 level from 21% to 2%. Meanwhile, modelled A-C_i and A-I_{inc} curves were slightly underestimated in low and middle N supply treatments when I_{inc} was higher than 500 μmol m^{-2} s^{-1} or C_a was kept higher than 400 μmol mol^{-1}, but overestimated when there was high N input (Fig. S2). Notably, both in maize and sorghum, the modelled A with response to C_i fluctuated under low and middle N input condition, as a result of fluctuations in the measured Φ_2 that were used as input to calculate J_{atp} for model fitting. Nonetheless, our results showed that overall, both C_3 and C_4 photosynthetic models fitted data well ($R^2 > 0.98$).

3.7. Sensitivity analysis

Fig. S3 shows the relative changes of the estimated J_{max} and V_{cmax} for C_3 species with up to ± 50% change in input parameter values. As expected, the enzyme-related pre-set parameters, like K_{mC}, K_{mO} and $S_{c/o}$ hardly had any influence on the estimates of J_{max} (Figs. S3a–c). V_{cmax} seemed to linearly change with K_{mC} (Fig. S3a). However, the linear change of V_{cmax} with K_{mO} and $S_{c/o}$ only existed when their values were lower than the pre-set values (Figs. S3b and c). Regarding the sensitivity to the previous estimated parameters, V_{cmax} and J_{max} hardly changed with R_d (Fig. S3d) while κ_{2LL} and T_p tended to have a slight influence on the estimates of V_{cmax} and J_{max} and δ changed the estimates of V_{cmax} significantly (Figs. S3e–g).

For C_4 species, the changes in pre-set and estimated parameters were mostly reflected in changes in χ_{gbs} (Fig. S4). Except for α, most of these parameters can have a noticeable influence on χ_{gbs} (Fig. S4). K_p and R_d can cause a notable change in g_m (Figs. S4c and g). The change in V_{cmax} was slightly affected by K_{mC}, K_{mO} and $S_{c/o}$ (Figs. S4a,b,d). Compared with other parameters, V_{pmax} was more likely to be influenced by K_p (Fig. S4c). n_b showed, not surprisingly, a systematic influence on the estimates of χ_{gbs} and the relationship between n_b and χ_{gbs} tended to be positively linear (Fig. S4f).

4. Discussion

Major cereal crops (rice, wheat, maize, and sorghum) grow on a global cultivation area of almost 700 million hectares, and supply approximately 50% of the world's caloric intake (Singer et al., 2019). In order to support smart farming, an accurate prediction of growth of major crops is essential. Photosynthesis is the primary process of crop growth and responds to variations in multiple environmental variables and management manipulations (in particular, N supply). The model of Farquhar et al. (1980) has been proven to be essential for modelling leaf photosynthesis in response to interactions of multiple physiological and environmental variables, and can be used as the basic model for upscaling to canopy and crop scales (Gu et al., 2014; Yin and Struik, 2017). However, reports about estimating and comparing photosynthetic parameters for these major crops together are quite rare, as most studies mainly focus on a single crop (e.g. Qian et al., 2012; Retta et al., 2016; Yin et al., 2009). Here, in our study, the primary photosynthetic parameters for four major crops, two C_3 species (rice and wheat) and two C_4 species (maize and sorghum) were quantified together. Although our estimated parameter values were subject to uncertainties in input constants of the FvCB model (Figs. S3 and S4), our results could serve as a referenced dataset in related research.

4.1. Effects of LNC on photosynthetic capacity

Photosynthetic capacity A_{max} has been found to be highly, positively correlated with LNC (Yoshida and Coronel, 1976), and R^2 for the linear regression is up to 0.80 (Field and Mooney, 1983). Furthermore, N related proxies have also been found to linearly increase with A_{max} under ambient or enhanced CO_2 condition, like leaf chlorophyll content ($R^2 >$ 0.95) (Wong, 1979). Our results showed that with an increase in LNC, the linear slopes of A_{max} to LNC were ranging from 14.71 to 30.83 μmol CO_2 g^{-1} N s^{-1} and, except for wheat, R^2 values were higher than 0.99 (Fig. 1). The steeper slope of A_{max} with respect to LNC in C_4 species is in line with earlier reports (Anten et al., 1995; Byrd et al., 1992; Sage and Pearcy, 1987). This is basically because of the higher efficiency of carboxylation of Rubisco associated with the CCM in the C_4 photosynthetic pathway (Black Jr, 1973; Schmitt and Edwards, 1981), as evidenced by the increased slope values for C_3 crops when O_2 was decreased to 2% (Fig. 1b).

4.2. Estimated biochemical parameters of photosynthetic capacity and their relationships with N

LNC significantly ($p < 0.001$) differed between C_3 and C_4 species. For example, LNC of rice was 1.6 times the value of maize (Table 3). V_{cmax}, J_{max} and T_p increased with increasing LNC (Harley et al., 1992b). Our results confirmed the linear increase of these photosynthetic parameters with LNC in rice and wheat (Fig. 5a–c). Values of V_{cmax} of rice and wheat tended to be higher than those of maize and sorghum at the same LNC (Fig. 5b), which may indicate that a lower amount of Rubisco is required in C_4 species for achieving the same rate of CO_2 assimilation as in C_3 species. The values of estimated J_{max} of rice and wheat varied from 73.3 to 343.1 μmol e^- m^{-2} s^{-1} under 21% and 2% O_2 conditions, higher than those of previous studies (Li et al., 2009; Yin et al., 2009). The LNC of wheat was significantly ($p < 0.01$) higher than that of rice, and this was compensated for by the significantly higher estimated χ_{Jmax} under 21% O_2 conditions in rice than in wheat. The lower χ_{Jmax} of wheat was in line with the small increment of A_{max} under high N condition (Fig. 1), which

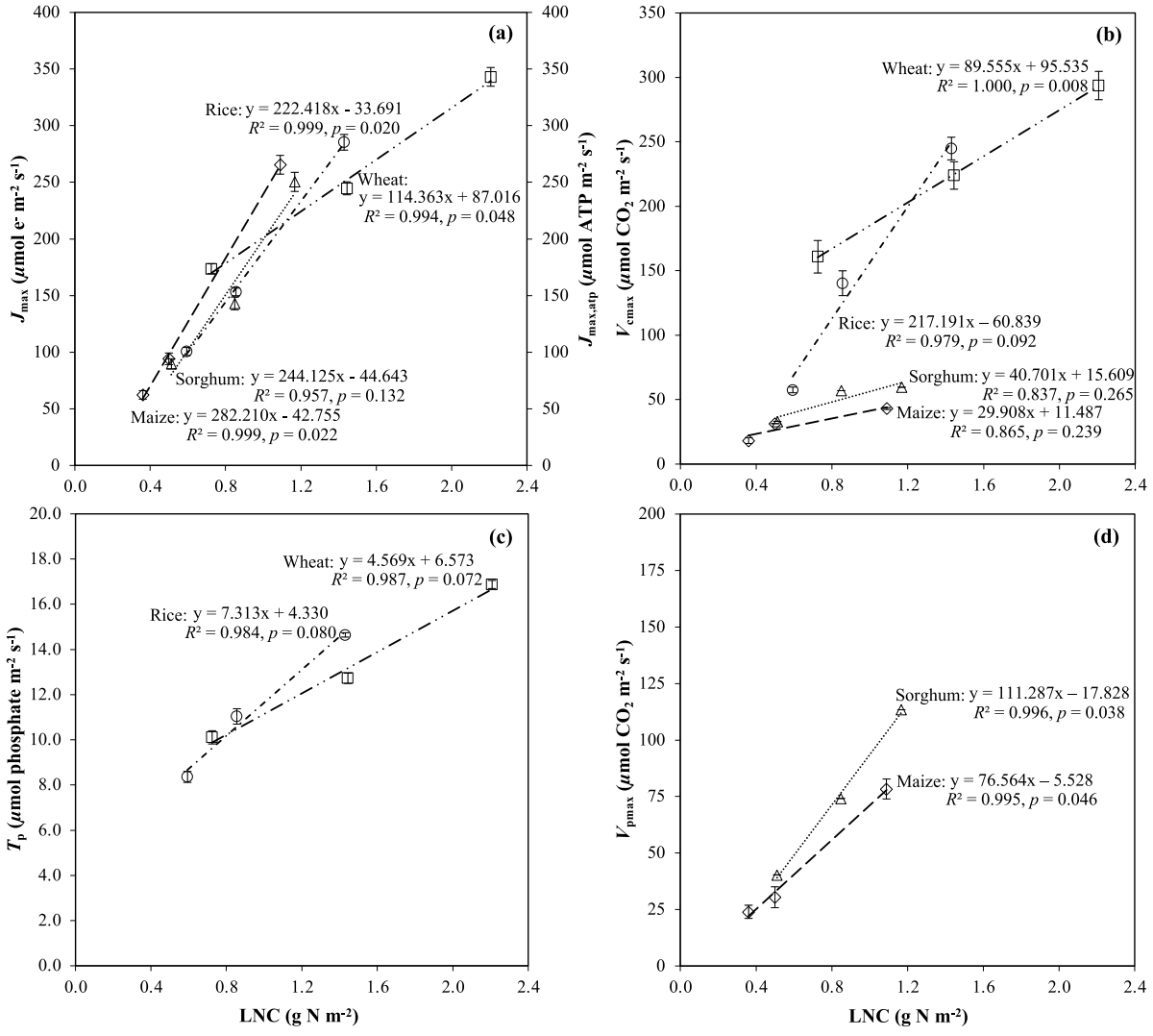

Fig. 5. Estimated maximum rate of linear electron transport J_{max} (for rice and wheat) or maximum rate of ATP production $J_{max,atp}$ (for maize and sorghum) (a), maximum rate of Rubisco carboxylation V_{cmax} (b), rate of triose phosphate utilization T_p (for rice and wheat) (c), and maximum rate of PEP carboxylation V_{pmax} (for maize and sorghum) (d) in relation to leaf nitrogen content (LNC) for rice (circles), wheat (squares), maize (diamonds) and sorghum (triangles) under 21% O_2 condition. Rice and wheat had different estimates of J_{max} under 21% and 2% O_2 levels (see the text), but in order to make them comparable with maize and sorghum, only J_{max} under 21% O_2 level is shown. Data points are shown with standard errors of the estimates.

indicates that the increasing trend of A with LNC would be ceased while plant growth is no longer limited by N supply (Hirose, 1984). For example, more than one third of the ability of carboxylation by Rubisco in wheat leaves would be inactivated once carboxylation excesses 155 μmol m^{-2} s^{-1}, although more N tends to be accumulated (Evans, 1983).

Estimated values of V_{cmax} for C_4 species ranged from 18.3 to 59.6 μmol CO_2 m^{-2} s^{-1} (Fig. 5b) and V_{pmax} varied from 24.0 to 113.4 μmol CO_2 m^{-2} s^{-1} (Fig. 5d), in line with earlier reports (Ghannoum et al., 2000) and both of them varied in proportion to LNC (Retta et al., 2016; Yin et al., 2011b). The estimated V_{pmax} also tended to have a higher value than V_{cmax} and the slopes of the regressed equation of V_{pmax} on LNC (χ_{Vpmax}) were 2.6 and 2.7 times values of χ_{Vcmax} in maize and sorghum, respectively (Fig. 5d). The higher V_{pmax} than V_{cmax} has also been observed in sugarcane when varying N supply ($V_{pmax} = 1.3V_{cmax}$) (Tofanello et al., 2021). Higher values of V_{pmax} than V_{cmax}, combined with a lower Michaelis-Menten constant value of PEPc than of Rubisco for CO_2 (Table 1), guarantees the faster C_4 cycle than the C_3 cycle, thereby, effectively sustaining the CCM in C_4 photosynthesis.

4.3. Estimations of R_d and its relationship with N

Environmental conditions also affect respiration. For instance, increased respiration rate of rice tends to be the primary cause of its yield losses under high temperature, while the photosynthetic rate hardly changed (Li et al., 2021). With respect to N response, earlier research has reported that leaf respiration occurring in the dark (R_{dk}) scales with LNC in several trees and shrubs (Ryan, 1995). Reich et al. (2008) demonstrated the strong relationship between R_{dk} and leaf N by utilizing a database containing 287 species. It has also been reported that the estimated R_d of maize generally increases with LNC (Retta et al., 2016). In our study, we also found R_d increased with N application and there was a linear relationship between R_d of C_3 and C_4 species and LNC, although the correlation was weaker for the C_4 species than for the C_3 species (Fig. 3b). Meanwhile, in line with the results in earlier reports that the estimated R_d of maize was higher than those of rice and wheat (Griffin and Turnbull, 2013; Yin et al., 2011a), we also found that the estimated R_d of sorghum, a common C_4 species, was also higher than the estimated R_d of rice and wheat (Fig. 3b). This is in contrary to the expectation that a higher observed LNC is supposed to lead to higher respiration costs (Mooney and Gulmon, 1982) as protein turnover represents a considerable expenditure of energy and thus associates with a significant proportion of leaf respiration (Penning de Vries, 1975). The reasons for higher R_d in C_4 than in C_3 crops need further studies to elucidate.

4.4. Estimation of g_m and g_{bs}

g_m may limit A by 20% in C_3 species (Warren, 2008). The analysis of our data using the variable J method (Harley et al., 1992a) confirmed that g_m of rice and wheat varied with C_i and I_{inc} (Fig. S1). The estimated g_m was lower than 0.8 mol m^{-2} s^{-1} (Fig. S1), in line with the results of von Caemmerer and Evans (2015) derived from the gas exchange and carbon isotope discrimination measurements. g_m of rice tended to be higher than that of wheat under different N supplies (Figs. S1 and 4a), compared with different g_m between the two crops reported by Ouyang et al. (2017). It has been found that there is a positive linear correlation between g_m and A_{max} ($R^2 = 0.84$) (von Caemmerer and Evans, 2015). We also found that g_m under the condition where A_{max} was measured tended to linearly increase with LNC (Fig. 4a). C_4 species has a higher g_m than C_3 species, because g_m in C_4 species arises from only the mesophyll cell-wall and plasma membrane resistance whereas g_m in C_3 species additionally includes resistance components from chloroplasts (Evans, 1996). In our estimates, g_m for maize and sorghum were 2.99 (0.65) and 1.87 (0.28) mol m^{-2} s^{-1}, respectively, similar to the estimates of Yin et al. (2011b) for maize.

Compared with g_m, g_{bs} is crucial in C_4 photosynthesis as it determines the efficiency of the CCM (Kromdijk et al., 2014) and tends to be more likely affected by pre-set model constants (Fig. S4). Under N deficient conditions, a low g_{bs} helps maintain high CO_2 concentration at Rubisco sites in compensation for the low PEPc activity (Tofanello et al., 2021). Our results also showed that estimated g_{bs} of maize and sorghum based on the assumed linear relationship of g_{bs} with LNC fitted data well, in line with the early reports about maize (Retta et al., 2016; Yin et al., 2011b). Like the observed difference of g_m in different C_3 species, g_{bs} varied between species as well and the estimated g_{bs} of sorghum was notably higher than the estimates for maize (Fig. 4b). A recent study showed that the increase in g_{bs} with LNC can hardly be explained by leaf anatomical traits, but is more likely associated with plasmodesmata density and membrane permeability (Retta et al., 2016). This is in line with the significantly enhanced expression of the plasma membrane intrinsic protein in *Cleome gynandra* (C_4) (Brautigam et al., 2011), which could confer higher permeability to CO_2 (Weber and von Caemmerer, 2010).

4.5. Implications of N response of photosynthetic parameters for smart crop management

Given the above-discussed crucial roles of N in affecting photosynthetic parameters and also considering the N effect on other aspects of crop growth, N management is central to precision cultivation of crops. Nitrogen management can be optimised with the diagnosis of crop N status. With well estimated photosynthetic parameters, crop models can predict real-time course of crop growth, thereby, potentially being able to support real-time crop N management.

Photosynthetic parameters may be estimated directly from exploring modern technologies. J_{max} has been directly retrieved from hyperspectral reflectance for quantifying seasonal and stressful photosynthetic changes (Lawson et al., 2020). Large seasonal and spatial variations in V_{cmax} have also been observed, especially for diverse crop rotation systems, based on the mapped global canopy V_{cmax} from 11 years of satellite chlorophyll fluorescence records (He et al., 2019). For instance, a higher V_{cmax} of winter wheat was observed in spring than V_{cmax} of maize in the summer in Shandong, China (He et al., 2019), in line with the differences of V_{cmax} for wheat and maize in our estimates (Fig. 5b). Nonetheless, until now, studies about directly estimating other photosynthetic parameters, such as T_p and V_{pmax}, or in other major field crops are scarce. However, methods to retrieve crop N status have been developed previously at different temporal and spatial resolutions from remote and proximal sensing images (Berger et al., 2020). By means of retrieving crop N, these key photosynthetic parameters can be indirectly retrieved from hyperspectral imagery based on our established correlation between photosynthetic parameters and LNC.

With the predicted photosynthetic parameters, photosynthetic capacity at the leaf level can be estimated. After up-scaling to the canopy photosynthesis, together with other growth and development processes, crop growth and its responses to weather, soil and field management can be estimated quantitatively by crop models. Correspondingly, according to actual crop growth status and predicted crop growth, the decisions of the adaptation of N fertilizer to the target yield or to environmental objectives can be made before the date of actual N applications. Thus, the identified relationship between estimated photosynthetic parameters and LNC in our study can serve for large scale photosynthetic parameter estimation by means of N retrieving from remote and proximal sensing images and be supportive the optimization of N management in smart crop cultivation. This is an area of our ongoing investigation.

5. Concluding remarks

We estimated photosynthetic parameters for four major crops, two C_3 species (rice and wheat) and two C_4 species (maize and sorghum), as well as their relationships with LNC. Our results showed that the estimates changed between C_3 and C_4 types, as well as between crops within each type. The significant relationships of these parameters with LNC can be used in crop models for the simulation of photosynthetic process from the

leaf to the canopy level. This, combined with the modelling of other growth processes, can help to bridge the gap between crop yield and retrieved crop N status from widely available hyperspectral data, and, therefore, may effectively support smart crop N management.

Authors' contribution

D.W. analyzed data and wrote the draft. W.R. and F.G. collected the data. P.E.L.v.d.P. managed the experiment. P.C.S. and X.Y. supervised the whole research process. All authors have approved the final version of the manuscript.

Data availability

The scripts used for the photosynthetic parameter fitting are available upon request to the corresponding author.

Declaration of competing interest

The authors declare that they have no competing interests. Author X. Yin (Editorial Board member) was not involved in the journal's review nor in decisions related to this manuscript.

Acknowledgements

Authors are grateful to the editor and two anonymous reviewers for their comments that allowed them to improve the manuscript.

List of abbreviations

ANCOVA	Analysis of covariance
A_{max}	maximum rate of light saturated assimilation at ambient CO_2 level
C_a	ambient CO_2 level
C_c	the CO_2 level at the carboxylating sites of Rubisco
C_i	the CO_2 level of substomatal cavity
CCM	CO_2-concentrating mechanism
F_m'	the maximum fluorescence yield
F_s	the steady-state fluorescence yield
FvCB model	the model of Farquhar, von Caemmerer & Berry (1980)
LNC	leaf nitrogen content (g N m^{-2})
PEP	phosphoenolpyruvate
PEPc	PEP carboxylase
PSII	Photosystem II
RUE	radiation use efficiency
TPU	triose phosphate utilization

Supplementary data

The supporting data to this article contain one supplementary table and four supplementary figures, and can be found online at https://doi.org/10.1016/j.crope.2022.05.004.

APPENDIX A. g_m model and the solution of A_c and A_j for C_3 species

Given that mesophyll diffusion conductance was identified as zero if light approaches zero (see Results), we used a simplified version of the variable-g_m model of Yin et al. (2009) without the terms for residual mesophyll diffusion conductance:

$$g_m = \delta(A + R_d)/(C_c - \Gamma_*) \quad \text{(A1)}$$

With this simplified form, parameter δ represents the carboxylation to mesophyll resistance ratio (Yin et al., 2020).

Combining Eqn (A1) with Eqn (1) and replacing C_c with ($C_i - A_c/g_m$) or ($C_i - A_j/g_m$), correspondingly, and then solving the quadratic equation for A_c and A_j gives:

$$A_c \text{ or } A_j = \left(-b - \sqrt{b^2 - 4ac}\right)\Big/(2a) \quad \text{(A2)}$$

where $a = x_2 + \Gamma_* + \delta(C_i + x_2)$

$$b = -\{(x_2 + \Gamma_*)(x_1 - R_d) + \delta(C_i + x_2)(x_1 - R_d) + \delta[x_1(C_i - \Gamma_*) - R_d(C_i + x_2)]\}$$

$$c = \delta(x_1 - R_d)[x_1(C_i - \Gamma_*) - R_d(C_i + x_2)]$$

where x_1 and x_2 are defined in eqn (1) in the main text.

APPENDIX B. The solution of A_{EE}, A_{ET}, A_{TE}, and A_{TT} for C_4 species

Combining Eqns (4)–(7) in the main text can solve the value A for each of these limitation combinations.

(1) If V_p is limited by the activity of PEPc (see Eqn (5a)), A_{EE} and A_{ET} can be solved as one of the roots of a standard cubic equation, which is suitable for calculating either A_{EE} or A_{ET} under any combinations of C_i, I_{inc} and O_i:

$$A_{EE}\ or\ A_{ET} = -2\sqrt{Q}cos(\psi/3) - p\Big/3 \tag{B1}$$

where $Q = (p^2 - 3q)/9$

$$\psi = cos^{-1}\left(U \Big/ \sqrt{Q^3}\right)$$

$$U = (2p^3 - 9pq + 27r)/54$$

in which, $p = m/(g_m + g_{bs} - x_2 g_m \alpha/0.047)$

$$q = n/(g_m + g_{bs} - x_2 g_m \alpha/0.047)$$

$$r = o/(g_m + g_{bs} - x_2 g_m \alpha/0.047)$$

and m, n and o are expressed as

$$m = d - (x_3 + x_2 O_i) g_m g_{bs} + (R_d - x_1)(g_m + g_{bs}) - (x_1 \gamma_* g_m + x_2 R_d g_m - x_2 k/g_{bs})\alpha/0.047$$

$$n = f + (x_3 + x_2 O_i)k + d(R_d - x_1) - g_m g_{bs}[x_1 \gamma_* O_i + R_d(x_3 + x_2 O_i)] + (x_1 \gamma_* + x_2 R_d)k\alpha/(0.047 g_{bs})$$

$$o = R_d[f + (x_3 + x_2 O_i)k] - x_1(f - k\gamma_* O_i)$$

and d, f and k are expressed as

$$d = g_m[R_m - V_{pmax} - C_i(g_m + 2g_{bs}) - K_p(g_m + g_{bs})]$$

$$f = g_m^2[C_i V_{pmax} + (C_i + K_p)(g_{bs} C_i - R_m)]$$

$$k = g_m^2 g_{bs}(C_i + K_p)$$

(2) If V_p is limited by electron transport (see Eqn (5b)), A_{TE} and A_{TT} can be solved as one of the roots of a generated quadratic equation:

$$A_{TE}\ or\ A_{TT} = \left(-b + \sqrt{b^2 - 4ac}\right)\Big/(2a) \tag{B2}$$

where $a = x_2 g_m \alpha/0.047 - g_m - g_{bs}$

$$b = g_m(C_i g_{bs} + V_p - R_m) + (x_3 + x_2 O_i) g_m g_{bs} + (x_1 \gamma_* + x_2 R_d) g_m \alpha/0.047 + (g_m + g_{bs})(x_1 - R_d)$$

$$c = -g_m(C_i g_{bs} + V_p - R_m)(x_1 - R_d) + g_m g_{bs}[x_1 \gamma_* O_i + R_d(x_3 + x_2 O_i)]$$

References

Anten, N.P.R., Schieving, F., Werger, M.J.A., 1995. Patterns of light and nitrogen distribution in relation to whole canopy carbon gain in C_3 and C_4 mono- and dicotyledonous species. Oecologia 101, 504–513.

Bailey-Serres, J., Parker, J.E., Ainsworth, E.A., Oldroyd, G.E.D., Schroeder, J.I., 2019. Genetic strategies for improving crop yields. Nature 575, 109–118.

Berger, K., Verrelst, J., Féret, J.-B., Wang, Z., Wocher, M., Strathmann, M., Danner, M., Mauser, W., Hank, T., 2020. Crop nitrogen monitoring: recent progress and principal developments in the context of imaging spectroscopy missions. Remote Sens. Environ. 242, 111758.

Bernacchi, C.J., Pimentel, C., Long, S.P., 2003. In vivo temperature response functions of parameters required to model RuBP-limited photosynthesis. Plant Cell Environ. 26, 1419–1430.

Bernacchi, C.J., Singsaas, E.L., Pimentel, C., Portis Jr., A.R., Long, S.P., 2001. Improved temperature response functions for models of Rubisco-limited photosynthesis. Plant Cell Environ. 25, 253–259.

Black Jr., C.C., 1973. Photosynthetic carbon fixation in relation to net CO_2 uptake. Annu. Rev. Plant Physiol. 24, 253–286.

Boote, K.J., Jones, J.W., Pickering, N.B., 1996. Potential uses and limitations of crop models. Agron. J. 88, 704–716.

Brautigam, A., Kajala, K., Wullenweber, J., Sommer, M., Gagneul, D., Weber, K.L., Carr, K.M., Gowik, U., Mass, J., Lercher, M.J., Westhoff, P., Hibberd, J.M., Weber, A.P., 2011. An mRNA blueprint for C_4 photosynthesis derived from

comparative transcriptomics of closely related C_3 and C_4 species. Plant Physiol. 155, 142–156.
Byrd, G.T., Sage, R.F., Brown, R.H., 1992. A comparison of dark respiration between C_3 and C_4 plants. Plant Physiol. 100, 191–198.
Chapman, K.S.R., Berry, J.A., Hatch, M.D., 1980. Photosynthetic metabolism in bundle sheath cells of the C_4 species *Zea mays*: sources of ATP and NADPH and the contribution of photosystem II. Arch. Biochem. Biophys. 202, 330–341.
Cousins, A.B., Ghannoum, O., von Caemmerer, S., Badger, M.R., 2010. Simultaneous determination of Rubisco carboxylase and oxygenase kinetic parameters in *Triticum aestivum* and *Zea mays* using membrane inlet mass spectrometry. Plant Cell Environ. 33, 444–452.
de Wit, C.T., 1978. Simulation of Assimilation, Respiration and Transpiration of Crops. PuDoc, Wageningen, The Netherlands.
Dubois, J.J.B., Fiscus, E.L., Booker, F.L., Flowers, M.D., Reid, C.D., 2007. Optimizing the statistical estimation of the parameters of the Farquhar–von Caemmerer–Berry model of photosynthesis. New Phytol. 176, 402–414.
Ehleringer, J.R., Sage, R.F., Flanagan, L.B., Pearcy, R.W., 1991. Climate change and the evolution of C_4 photosynthesis. Trends Ecol. Evol. 6, 95–99.
Evans, J.R., 1983. Nitrogen and photosynthesis in the flag leaf of wheat (*Triticum aestivum* L.). Plant Physiol. 72, 297–302.
Evans, J.R., 1996. Developmental constraints on photosynthesis: effects of light and nutrition. In: Baker, N.R. (Ed.), Photosynthesis and the Environment. Kluwer, Dordrecht, pp. 281–304.
Evans, J.R., Clarke, V.C., 2019. The nitrogen cost of photosynthesis. J. Exp. Bot. 70, 7–15.
Evans, J.R., von Caemmerer, S., 1996. Carbon dioxide diffusion inside leaves. Plant Physiol. 110, 339–346.
Farquhar, G.D., von Caemmerer, S., Berry, J.A., 1980. A biochemical model of photosynthetic CO_2 assimilation in leaves of C_3 species. Planta 149, 78–90.
Field, C., Mooney, H.A., 1983. Leaf age and seasonal effects on light, water, and nitrogen use efficiency in a California shrub. Oecologia 56, 348–355.
Flexas, J., Diaz-Espejo, A., Berry, J.A., Cifre, J., Galmes, J., Kaldenhoff, R., Medrano, H., Ribas-Carbo, M., 2007. Analysis of leakage in IRGA's leaf chambers of open gas exchange systems: quantification and its effects in photosynthesis parameterization. J. Exp. Bot. 58, 1533–1543.
Genty, B., Briantais, J.-M., Baker, N.R., 1989. The relationship between the quantum yield of photosynthetic electron transport and quenching of chlorophyll fluorescence. Biochim. Biophys. Acta 990, 87–92.
Ghannoum, O., von Caemmerer, S., Ziska, L.H., Conroy, J.P., 2000. The growth response of C_4 plants to rising atmospheric CO_2 partial pressure: a reassessment. Plant Cell Environ. 23, 931–942.
Griffin, K.L., Turnbull, M.H., 2013. Light saturated RuBP oxygenation by Rubisco is a robust predictor of light inhibition of respiration in *Triticum aestivum* L. Plant Biol. 15, 769–775.
Gu, J., Yin, X., Stomph, T.J., Struik, P.C., 2014. Can exploiting natural genetic variation in leaf photosynthesis contribute to increasing rice productivity? A simulation analysis. Plant Cell Environ. 37, 22–34.
Hank, T.B., Berger, K., Bach, H., Clevers, J.G.P.W., Gitelson, A., Zarco-Tejada, P., Mauser, W., 2019. Spaceborne imaging spectroscopy for sustainable agriculture: contributions and challenges. Surv. Geophys. 40, 515–551.
Harley, P.C., Loreto, F., Di Marco, G., Sharkey, T.D., 1992a. Theoretical considerations when estimating the mesophyll conductance to CO_2 flux by analysis of the response of photosynthesis to CO_2. Plant Physiol. 98, 1429–1436.
Harley, P.C., Thomas, R.B., Reynolds, J.F., Strain, B.R., 1992b. Modelling photosynthesis of cotton grown in elevated CO_2. Plant Cell Environ. 15, 271–282.
He, L., Chen, J.M., Liu, J., Zheng, T., Wang, R., Joiner, J., Chou, S., Chen, B., Liu, Y., Liu, R., Rogers, C., 2019. Diverse photosynthetic capacity of global ecosystems mapped by satellite chlorophyll fluorescence measurements. Remote Sens. Environ. 232, 111344.
Herold, A., 1980. Regulation of photosynthesis by sink activity-the missing link. New Phytol. 86, 131–144.
Hirose, T., 1984. Nitrogen use efficiency in growth of *Polygonum cuspidatum* Sieb. et Zucc. Ann. Bot. 54, 695–704.
Kanai, R., Edwards, G.E., 1999. The biochemistry of C_4 photosynthesis. In: Sage, R.F., Monson, R.K. (Eds.), C_4 Plant Biology. Academic Press, Toronto, pp. 49–87.
Kiniry, J.R., Jones, C.A., O'Toole, J.C., Blanchet, R., Cabelguenne, M., Spanel, D.A., 1989. Radiation-use efficiency in biomass accumulation prior to grain-filling for five grain-crop species. Field Crops Res. 20, 51–64.
Kromdijk, J., Ubierna, N., Cousins, A.B., Griffiths, H., 2014. Bundle-sheath leakiness in C_4 photosynthesis: a careful balancing act between CO_2 concentration and assimilation. J. Exp. Bot. 65, 3443–3457.
Laisk, A., Oja, V., Rasulov, B., Ramma, H., Eichelmann, H., Kasparova, I., Pettai, H., Padu, E., Vapaavuori, E., 2002. A computer-operated routine of gas exchange and optical measurements to diagnose photosynthetic apparatus in leaves. Plant Cell Environ. 25, 923–943.
Lawlor, D.W., 1995. Photosynthesis, productivity and environment. J. Exp. Bot. 46, 1449–1461.
Lawson, T., Bernacchi, C., Driever, S., Pederson, T., Dracup, E., Guan, K., Ainsworth, E., Montes, C.M., Serbin, S., Wu, J., Fu, P., Meacham-Hensold, K., 2020. Plot-level rapid screening for photosynthetic parameters using proximal hyperspectral imaging. J. Exp. Bot. 71, 2312–2328.
Leegood, R.C., von Caemmerer, S., 1989. Some relationships between contents of photosynthetic intermediates and the rate of photosynthetic carbon assimilation in leaves of *Zea mays* L. Planta 178, 258–266.
Li, G., Chen, T., Feng, B., Peng, S., Tao, L., Fu, G., 2021. Respiration, rather than photosynthesis, determines rice yield loss under moderate high-temperature conditions. Front. Plant Sci. 12, 678653.
Li, T., Hasegawa, T., Yin, X., Zhu, Y., Boote, K., Adam, M., Bregaglio, S., Buis, S., Confalonieri, R., Fumoto, T., Gaydon, D., Marcaida, M., Nakagawa, H., Oriol, P., Ruane, A.C., Ruget, F., Singh, B., Singh, U., Tang, L., Tao, F., Wilkens, P., Yoshida, H., Zhang, Z., Bouman, B., 2015. Uncertainties in predicting rice yield by current crop models under a wide range of climatic conditions. Global Change Biol. 21, 1328–1341.
Li, Y., Gao, Y., Xu, X., Shen, Q., Guo, S., 2009. Light-saturated photosynthetic rate in high-nitrogen rice (*Oryza sativa L.*) leaves is related to chloroplastic CO_2 concentration. J. Exp. Bot. 60, 2351–2360.
Loreto, F., Harley, P.C., Di Marco, G., Sharkey, T.D., 1992. Estimation of mesophyll conductance to CO_2 flux by three different methods. Plant Physiol. 98, 1437–1443.
Loriaux, S.D., Avenson, T.J., Welles, J.M., McDermitt, D.K., Eckles, R.D., Riensche, B., Genty, B., 2013. Closing in on maximum yield of chlorophyll fluorescence using a single multiphase flash of sub-saturating intensity. Plant Cell Environ. 36, 1755–1770.
McDowell, N.G., 2011. Mechanisms linking drought, hydraulics, carbon metabolism, and vegetation mortality. Plant Physiol. 155, 1051–1059.
Monteith, J.L., 1977. Climate and the efficiency of crop production in Britain. Philos. T. Roy. Soc. B. 281, 277–294.
Mooney, H.A., Gulmon, S.L., 1982. Constraints on leaf structure and function in reference to herbivory. Bioscience 32, 198–206.
Niinemets, Ü., Tenhunen, J.D., 1997. A model separating leaf structural and physiological effects on carbon gain along light gradients for the shade-tolerant species *Acer saccharum*. Plant Cell Environ. 20, 845–866.
Osmond, C.B., Winter, K., Ziegler, H., 1982. Physiological plant ecology II. In: Lange, O.L., Nobel, P.S., Osmond, C.B., Ziegler, H. (Eds.), Encyclopedia of Plant Physiology. Springer-Verlag, Berlin Heidelberg New York, pp. 479–547.
Ouyang, W., Struik, P.C., Yin, X., Yang, J., 2017. Stomatal conductance, mesophyll conductance, and transpiration efficiency in relation to leaf anatomy in rice and wheat genotypes under drought. J. Exp. Bot. 68, 5191–5205.
Penning de Vries, F.W.T., 1975. The cost of maintenance processes in plant cells. Ann. Bot. 39, 77–92.
Pingali, P.L., 2012. Green revolution: impacts, limits, and the path ahead. Proc. Natl. Acad. Sci. U.S.A. 109, 12302–12308.
Qian, T., Elings, A., Dieleman, J.A., Gort, G., Marcelis, L.F.M., 2012. Estimation of photosynthesis parameters for a modified Farquhar–von Caemmerer–Berry model using simultaneous estimation method and nonlinear mixed effects model. Environ. Exp. Bot. 82, 66–73.
R Core Team, 2021. R: A Language and Environment for Statistical Computing. R Foundation for Statistical Computing, Vienna.
Reich, P.B., Tjoelker, M.G., Pregitzer, K.S., Wright, I.J., Oleksyn, J., Machado, J.L., 2008. Scaling of respiration to nitrogen in leaves, stems and roots of higher land plants. Ecol. Lett. 11, 793–801.
Retta, M., Yin, X., van der Putten, P.E., Cantre, D., Berghuijs, H.N., Ho, Q.T., Verboven, P., Struik, P.C., Nicolai, B.M., 2016. Impact of anatomical traits of maize (*Zea mays* L.) leaf as affected by nitrogen supply and leaf age on bundle sheath conductance. Plant Sci. 252, 205–214.
Rogers, A., 2014. The use and misuse of $V_{c,max}$ in earth system models. Photosynth. Res. 119, 15–29.
Ryan, M.G., 1995. Foliar maintenance respiration of subalpine and boreal trees and shrubs in relation to nitrogen content. Plant Cell Environ. 18, 765–772.
Sage, R.F., Pearcy, R.W., 1987. The nitrogen use efficiency of C_3 and C_4 plants: II. Leaf nitrogen effects on the gas exchange characteristics of *Chenopodium album* (L.) and *Amaranthus retroflexus* (L.). Plant Physiol. 84, 959–963.
Schmitt, M.R., Edwards, G.E., 1981. Photosynthetic capacity and nitrogen use efficiency of maize, wheat, and rice: a comparison between C_3 and C_4 photosynthesis. J. Exp. Bot. 32, 459–466.
Sharkey, T.D., Bernacchi, C.J., Farquhar, G.D., Singsaas, E.L., 2007. Fitting photosynthetic carbon dioxide response curves for C_3 leaves. Plant Cell Environ. 30, 1035–1040.
Sinclair, T.R., Horie, T., 1989. Leaf nitrogen, photosynthesis, and crop radiation use efficiency: a review. Crop Sci. 29, 90–98.
Sinclair, T.R., Muchow, R.C., 1999. Radiation use efficiency. Adv. Agron. 65, 215–265.
Sinclair, T.R., Rawlins, S.L., 1993. Inter-seasonal variation in soybean and maize yields under global environmental change. Agron. J. 85, 406–409.
Singer, S.D., Foroud, N.A., Laurie, J.D., 2019. Molecular Improvement of Grain: Target Traits for a Changing World. Elsevier, Oxford.
Tofanello, V.R., Andrade, L.M., Flores-Borges, D.N.A., Kiyota, E., Mayer, J.L.S., Creste, S., Machado, E.C., Yin, X., Struik, P.C., Ribeiro, R.V., 2021. Role of bundle sheath conductance in sustaining photosynthesis competence in sugarcane plants under nitrogen deficiency. Photosynth. Res. 149, 275–287.
Valentini, R., Epron, D., de Angelis, P., Matteucci, G., Dreyer, E., 1995. *In situ* estimation of net CO_2 assimilation, photosynthetic electron flow and photorespiration in Turkey oak (*Q. cerris* L.) leaves: diurnal cycles under different levels of water supply. Plant Cell Environ. 18, 631–640.
von Caemmerer, S., 2000. Biochemical Models of Leaf Photosynthesis. CSIRO Publishing, Melbourne.
von Caemmerer, S., Evans, J.R., 2015. Temperature responses of mesophyll conductance differ greatly between species. Plant Cell Environ. 38, 629–637.
von Caemmerer, S., Evans, J.R., Hudson, G.S., Andrews, T.J., 1994. The kinetics of ribulose-1,5-bisphosphate carboxylase/oxygenase in vivo inferred from measurements of photosynthesis in leaves of transgenic tobacco. Planta 195, 88–97.
von Caemmerer, S., Furbank, R.T., 1999. Modelling C_4 photosynthesis. In: Sage, R.F., Monson, R.K. (Eds.), C_4 Plant Biology. Academic Press, Toronto, pp. 173–211.
Walter, A., Finger, R., Huber, R., Buchmann, N., 2017. Opinion: smart farming is key to developing sustainable agriculture. Proc. Natl. Acad. Sci. U.S.A. 114, 6148–6150.

Warren, C.R., 2008. Does growth temperature affect the temperature responses of photosynthesis and internal conductance to CO_2? A test with Eucalyptus regnans. Tree Physiol. 28, 11–19.
Weber, A.P.M., von Caemmerer, S., 2010. Plastid transport and metabolism of C_3 and C_4 plants—comparative analysis and possible biotechnological exploitation. Curr. Opin. Plant Biol. 13, 256–264.
Wong, S.C., 1979. Elevated atmospheric partial pressure of CO_2 and plant growth. I. Interactions of nitrogen nutrition and photosynthetic capacity in C_3 and C_4 plants. Oecologia 44, 68–74.
Yin, X., Busch, F.A., Struik, P.C., Sharkey, T.D., 2021a. Evolution of a biochemical model of steady-state photosynthesis. Plant Cell Environ. 44, 2811–2837.
Yin, X., Struik, P.C., 2012. Mathematical review of the energy transduction stoichiometries of C_4 leaf photosynthesis under limiting light. Plant Cell Environ. 35, 1299–1312.
Yin, X., Struik, P.C., 2017. Can increased leaf photosynthesis be converted into higher crop mass production? A simulation study for rice using the crop model GECROS. J. Exp. Bot. 68, 2345–2360.
Yin, X., Struik, P.C., Goudriaan, J., 2021b. On the needs for combining physiological principles and mathematics to improve crop models. Field Crops Res. 271, 108254.
Yin, X., Struik, P.C., Romero, P., Harbinson, J., Evers, J.B., van der Putten, P.E.L., Vos, J., 2009. Using combined measurements of gas exchange and chlorophyll fluorescence to estimate parameters of a biochemical C_3 photosynthesis model: a critical appraisal and a new integrated approach applied to leaves in a wheat (*Triticum aestivum*) canopy. Plant Cell Environ. 32, 448–464.
Yin, X., Sun, Z., Struik, P.C., Gu, J., 2011a. Evaluating a new method to estimate the rate of leaf respiration in the light by analysis of combined gas exchange and chlorophyll fluorescence measurements. J. Exp. Bot. 62, 3489–3499.
Yin, X., Sun, Z., Struik, P.C., van der Putten, P.E.L., van Ieperen, W., Harbinson, J., 2011b. Using a biochemical C_4 photosynthesis model and combined gas exchange and chlorophyll fluorescence measurements to estimate bundle-sheath conductance of maize leaves differing in age and nitrogen content. Plant Cell Environ. 34, 2183–2199.
Yin, X., van der Putten, P.E.L., Belay, D., Struik, P.C., 2020. Using photorespiratory oxygen response to analyse leaf mesophyll resistance. Photosynth. Res. 144, 85–99.
Yoshida, S., Coronel, V., 1976. Nitrogen nutrition, leaf resistance, and leaf photosynthetic rate of the rice plant. Soil Sci. Plant Nutr. 22, 207–211.